Fungal Metabolites. XX.[1,2] Effect of Proline Residue on the Structure of Ion-Channel-Forming Peptide, Trichosporin B-VIa

Yasuo NAGAOKA,[a] Akira IIDA,[a] Eiichi TACHIKAWA,[b] and Tetsuro FUJITA*,[a]

Faculty of Pharmaceutical Sciences, Kyoto University,[a] Sakyo-ku, Kyoto 606–01, Japan and School of Medicine, Iwate Medical University,[b] Morioka 020, Japan. Received February 27, 1995; accepted April 10, 1995

The secondary structures of an ion-channel-forming icosapeptaibol, trichosporin B-VIa, and its Aib^{14}-substituted derivative containing no Pro were investigated on the basis of CD and various NMR experiments in methanol. Trichosporin B-VIa has a fully helical structure with a kink stabilized by a 1←4 hydrogen-bond between the Leu^{12} CO and Val^{15} NH. The helical structure is composed of 3_{10}-helix in the N-terminal first turn and the C-terminal moiety following Leu^{12}, and α-helix in the middle region. In contrast, the Aib^{14} derivative predominantly has a straight α-helical structure except for a 3_{10}-helix region in the N-terminal first turn.

Key words *Trichoderma polysporum*; peptaibol; trichosporin; α-aminoisobutyric acid; ion-channel

Trichosporin Bs (TS-Bs)[3,4] are peptides isolated from the culture broth of the fungus *Trichoderma polysporum*. (LINK *ex* PERS.) RIFAI (strain TMI 60146). These peptides contain a high proportion of α-aminoisobutyric acid (Aib) and their N- and C-terminal residues are protected by an acetyl group (Ac) and phenylalaninol (Pheol), respectively. On the basis of these characteristics, TS-Bs are members of the peptaibol family.[5] They show biological activities such as uncoupling of oxidative phosphorylation in rat liver mitochondria[6] and induction of catecholamine secretion from bovine adrenal medullary chromaffin cells.[7] These bioactivities are related to an alteration of ion permeability through biomembranes, suggesting that TS-Bs form ion-channels in the membranes or modify the membranes. Recently, we found that TS-B-VIa, one of the major components of TS-Bs, forms ion-channels in planar lipid bilayers,[8] as other peptaibols do. Many peptaibols, *e.g.* alamethicins,[9] suzukacillins,[10] paracelsins,[5] trichorzianines,[11] hypelcins,[12] and trichocellins,[13] have a Pro residue at the seventh position from the C-terminal. This Pro residue generates a kinked structure[14–16] which is supposed to play an important role in voltage-gated ion-channel formation.[14]

To examine the role of Pro^{14} in the structure and function of peptaibols, TS-B-VIa was derived to Aib^{14}-TS-B-VIa, in which Pro in TS-B-VIa is replaced by Aib.[17] TS-B-VIa and Aib^{14}-TS-B-VIa have the following primary structures: TS-B-VIa (Aib^{14}-TS-B-VIa), Ac–Aib–Ala–Aib–Ala–Aib–Aib–Gln–Aib–Ile–Aib–Gly–Leu–Aib–Pro(Aib)–Val–Aib–Aib–Gln–Gln–Pheol. In this paper, we describe the solution structures of these peptides.

Materials and Methods

Synthetic TS-B-VIa and Aib^{14}-TS-B-VIa[17] were used for the experiments. CD spectra were recorded at 23 °C on a JASCO J-720 spectropolarimeter using a 1-mm path cell. For NMR measurements, samples were dissolved in CD_3OH, containing TMS as an internal standard. All ^{1}H-NMR spectra were recorded by a Bruker AM-600 (600 MHz) spectrometer. DQF-COSY spectra[18] were measured in the phase-sensitive mode with selective saturation of the OH resonance of the solvent at all times. A total of 512 t_1-values were recorded, with 2048 data points and 32 scans for each t_1. NOESY spectra[19] were measured in the phase-sensitive mode with selective saturation of the OH resonance of the solvent at all times except during the detection periods. A total of 512 t_1-values were recorded, with 2048 data points and 64 scans for each t_1. The data matrices of DQF-COSY and NOESY were filtered by shifted squared sine-bell multiplication in the t_1 and t_2 dimensions and zero-filled to 2048 data points in the t_1 dimension; spectral width 6000 Hz; relaxation delay time 2.4 s. For NOESY, the mixing time was 300 ms with 10% random variation. The spectra were unsymmetrized. Under the NMR conditions, there was no evidence for peptide aggregation: no broadening of signals or significant variations of chemical shifts were detectable in the concentration range from 5 to 40 mM and in the temperature range from 268 to 307 K.

Results and Discussion

As shown in Fig. 1, the CD spectra of TS-B-VIa and Aib^{14}-TS-B-VIa in methanol were characteristic of right-handed helices. The ellipticities of Aib^{14}-TS-B-VIa at 208 and 222 nm were greater than those of TS-B-VIa, indicating that the replacement of Pro with Aib increased the helical content of the molecule. In our previous work, a similar increment of helicity was observed in des-Pro^{14}-TS-B-V,[16] a synthetic 19-residue analogue of TS-B-V without the Pro^{14} residue. These increments of helicity are consistent with the fact that Aib promotes helical conformation and Pro often breaks it.[20,21]

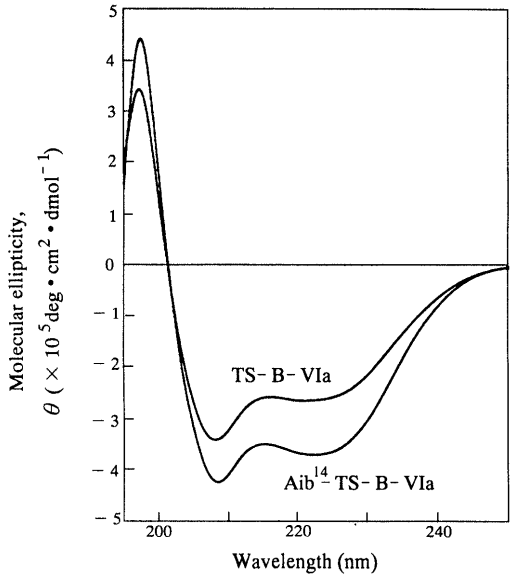

Fig. 1. CD Spectra of TS-B-VIa and Aib^{14}-TS-B-VIa in MeOH (25 °C)

Molecular ellipticity, θ (deg cm^2 dmol^{-1}), at 208 and 222 nm: -3.415×10^5 and -2.639×10^5 (TS-B-VIa), -4.219×10^5 and -3.706×10^5 (Aib^{14}-TS-B-VIa).

* To whom correspondence should be addressed.

© 1995 Pharmaceutical Society of Japan

NII-Electronic Library Service

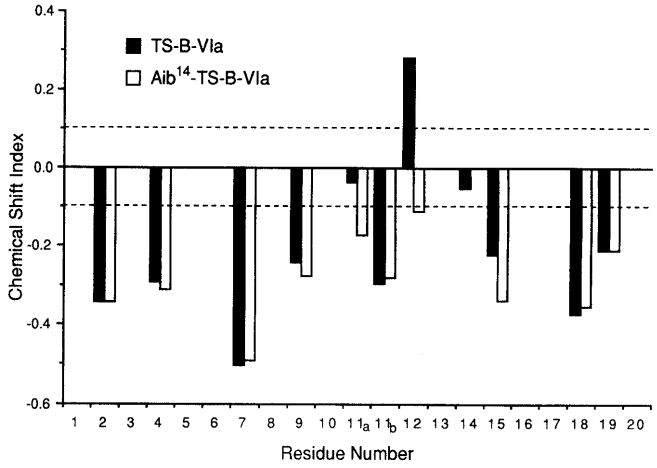

Fig. 2. Comparison of Chemical Shift Index Values between TS-B-VIa and Aib^{14}-TS-B-VIa

Chemical shift index is the difference between CαH chemical shift values for α-amino acid residues of the peptides (described in a previous paper[14]) and those in a random coil conformation, described by Wishart *et al.*[22]

The secondary structure of a protein can be estimated from the "chemical shift index," the difference between the CαH chemical shift in a protein structure and that in a random coil.[22] When the chemical shift indices are consecutively less than −0.1 ppm for more than four residues, the structure in that part is considered to be a helix, while more than three consecutive values greater than +0.1 ppm suggest a β-strand. Termination points of helices or β-strands are indicated by the appearance of chemical shift indices that are opposite in magnitude to those of the corresponding secondary structure or by the first appearance of two consecutive values within ±0.1 ppm. Figure 2 shows the chemical shift indices calculated for TS-B-VIa and Aib^{14}-TS-B-VIa. Because of the lack of an α proton in Aib, the values for Aib residues are not marked. The results suggested that a helical structure in the N-terminal moiety of TS-B-VIa terminated at Gly^{11} and another helical structure was located in the C-terminal part from Val^{15}. On the other hand, all the chemical shift index values of Aib^{14}-TS-B-VIa were less than −0.1 ppm, suggesting that the Aib^{14}-TS-B-VIa molecule has a regular helical structure all over the sequence. These structures for TS-B-VIa and Aib^{14}-TS-B-VIa were in agreement with those obtained from *J* values reported previously.[17]

In order to obtain detailed structural information, NOESY spectra of both peptides (40 mM) were recorded in CD_3OH (Fig. 3). In the spectra for both peptides, successive NOEs [$d_{NN}(i, i+1)$-type] and other diagnostic NOEs [$d_{\alpha N}(i, i+1)$-, $d_{\alpha N}(i, i+3)$-, $d_{\alpha\beta}(i, i+3)$- and $d_{\beta N}(i, i+1)$-type] strongly suggested overall helical structure (Fig. 4).[23] Characteristic NOEs [$d_{\alpha N}(i, i+4)$-, $d_{\alpha\beta}(i, i+3)$-, and $d_{\alpha N}(i, i+2)$-type] were also observed in both peptides. These NOEs are generally used to distinguish between α-helix and 3_{10}-helix: in an ideal α-helical peptide, $d_{\alpha N}(i, i+4)$- and $d_{\alpha\beta}(i, i+3)$-type NOEs are stronger and $d_{\alpha N}(i, i+2)$-type NOEs are weaker or cannot be observed, while in an ideal 3_{10}-helical structure, stronger $d_{\alpha N}(i, i+2)$-type NOEs are observed.[24] In the N-terminal region of TS-B-VIa, a strong $d_{\alpha N}(i, i+2)$ (between the acetyl CH_3 proton and the Ala^2 NH proton) and a strong $d_{\alpha N}(i, i+4)$ (between the acetyl CH_3 proton and the Ala^4 NH proton) were observed spontaneously (Figs. 3a, 4a). Therefore, the N-terminal first turn of TS-B-VIa was considered as a mixed conformation of 3_{10}- and α-helix. In the region from position 4 of TS-B-VIa, a stretch of α-helix was indicated by strong or medium [$d_{\alpha N}(i, i+4)$, $i=4, 9$] and [$d_{\alpha\beta}(i, i+3)$, $i=4, 9$], and terminated at position 11, because the $d_{\alpha N}(i, i+4)$ between the Gly^{11} αH and Val^{15} NH, or between the Leu^{12} αH and Aib^{16} NH were absent (Figs. 3a, 4a). In the C-terminal region following Pro^{14} of TS-B-VIa, [$d_{\alpha N}(i, i+2)$, $i=14, 15$] were much stronger than [$d_{\alpha N}(i, i+4)$, $i=14, 15$] (Figs. 3a, 4a). Therefore, the C-terminal region (positions 14 to 20) of TS-B-VIa takes predominantly a 3_{10}-helical conformation. However, the weaker [$d_{\alpha N}(i, i+4)$ $i=14, 15$] in this 3_{10}-helical region suggested that the 3_{10}-helix is not tightly bound and has a larger radius and a smaller pitch than those of the ideal 3_{10}-helix. It is interesting that in our previous work on TS-B-V, a member of TS-Bs, we found that the C-terminal moiety has α-helical conformation.[16] The conformational difference between TS-B-VIa and TS-B-V could be due to the influence of position 3 (Aib in TS-B-VIa, Ala in TS-B-V).

In Aib^{14}-TS-B-VIa, the N-terminal first turn has a mixed 3_{10}- and α-helical structure, as in TS-B-VIa (Figs. 3b, 4b). In the other part, strong or medium $d_{\alpha N}(i, i+4)$ and $d_{\alpha\beta}(i, i+3)$ cross peaks were observed, indicating that α-helical structure is predominant in this region. Thus, the conformation of Aib^{14}-TS-B-VIa can be regarded as a straight cylinder.

The kinetics of proton-deuterium (H-D) exchange between backbone NH and deuterium ions in the solvent provides information on the flexibility of backbone hydrogen-bonds (H-bond).[25] The H-D exchange rates of both peptides are shown in Fig. 5. The exchange rates of positions 1 to 12 are similar for both peptides, suggesting that the conformations of these peptides are almost identical in this region. The very high exchange rates for the N-terminal Aib^1 NH and Ala^2 NH (Fig. 5a) indicated that these protons are not involved in intramolecular H-bonding and are always exposed to the solvent. The low rates for the Aib^3 NHs and Ala^4 NHs of both peptides supported the presence of two types of H-bonds, as indicated by the NOE data: i) a 1←4 H-bond between the acetyl CO and the Aib^3 NH (3_{10}-helical turn) and ii) a 1←5 H-bond between the acetyl CO and the Ala^4 NH (α-helical turn). The rates for positions 5 to 20 of both peptides were low enough to imply that all the NHs in this region participate in inter-residual H-bonding. The Val^{15} NH and the Aib^{16} NH of TS-B-VIa should participate in H-bonding with the Leu^{12} CO and Aib^{13} CO, respectively, because the 1←5 H-bonding between the Gly^{11} CO and Val^{15} NH or between the Leu^{12} CO and Aib^{16} NH is ruled out by the NOE data. However, the H-D exchange rate for the Aib^{16} NH of TS-B-VIa was faster than those of other NHs except for the N-terminal NHs (Fig. 5), suggesting that the H-bonding of this NH is not so tight and this residue may be exposed to the solvent. Accordingly, the 1←4 H-bonding between the Leu^{12} CO and the Val^{15} NH would stabilize the Pro-

NII-Electronic Library Service

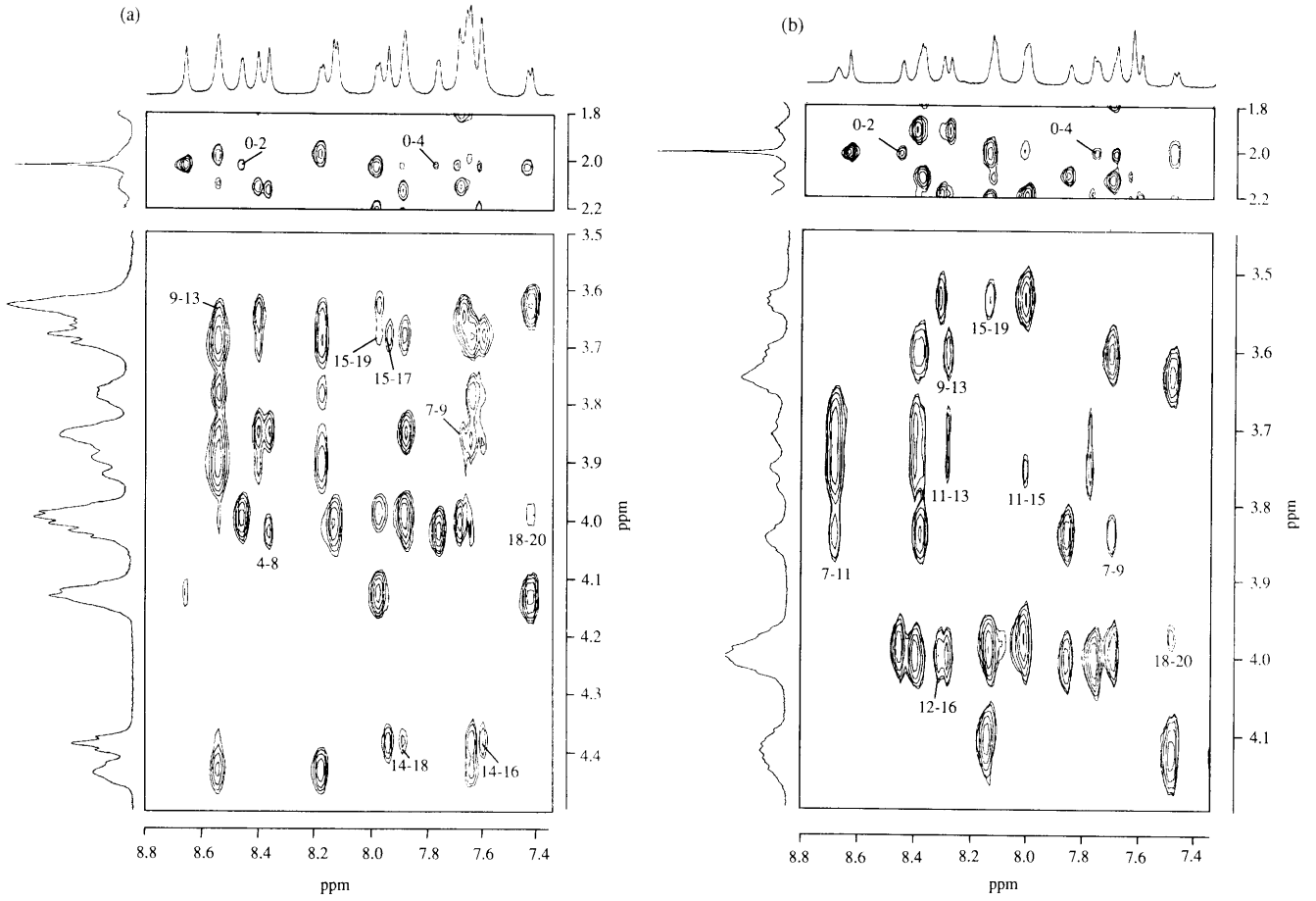

Fig. 3. Parts of the 600 MHz NOESY Spectra of 40 mM TS-B-VIa (a) and 40 mM Aib[14]-TS-B-VIa (b) in CD_3OH at 268 K, with a Mixing Time of 300 ms

NOE cross-peaks [$d_{\alpha N}(i, i+2)$ or $d_{\alpha N}(i, i+4)$] are labeled with the numbers of two residues involving acetyl CH_3 (0). In order to enhance the NOEs, NOESY spectra were recorded at low temperature (268 K) and the signals have been assigned by means of the same procedures as described in the previous paper.[17]

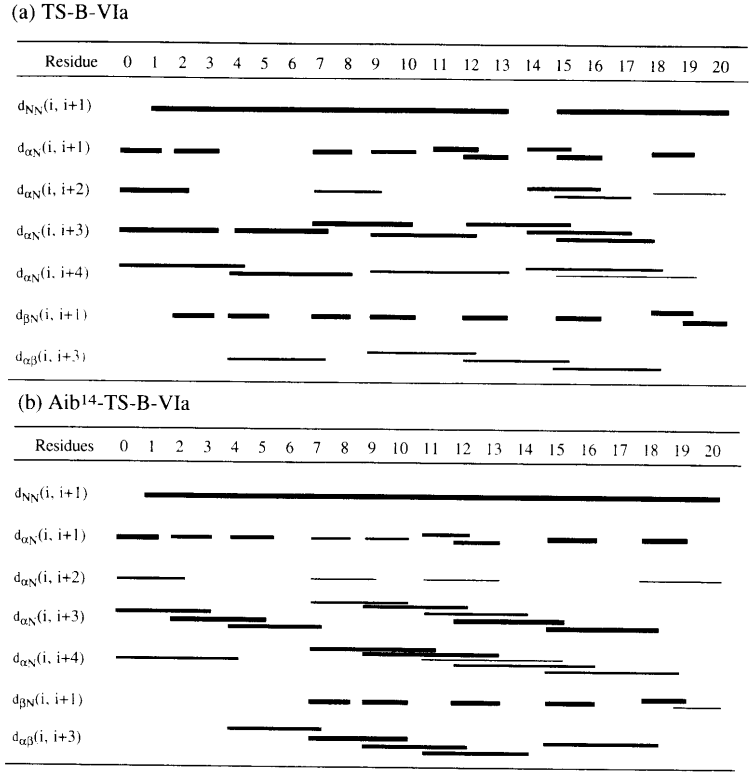

Fig. 4. Inter-Residual NOEs Observed in CD_3OH at 268 K for TS-B-VIa (a) and Aib[14]-TS-B-VIa (b)

The observed NOEs are classified based on the cross-peak counter levels (represented by the thickness of the lines). Residue 0 represents the acetyl group.

NII-Electronic Library Service

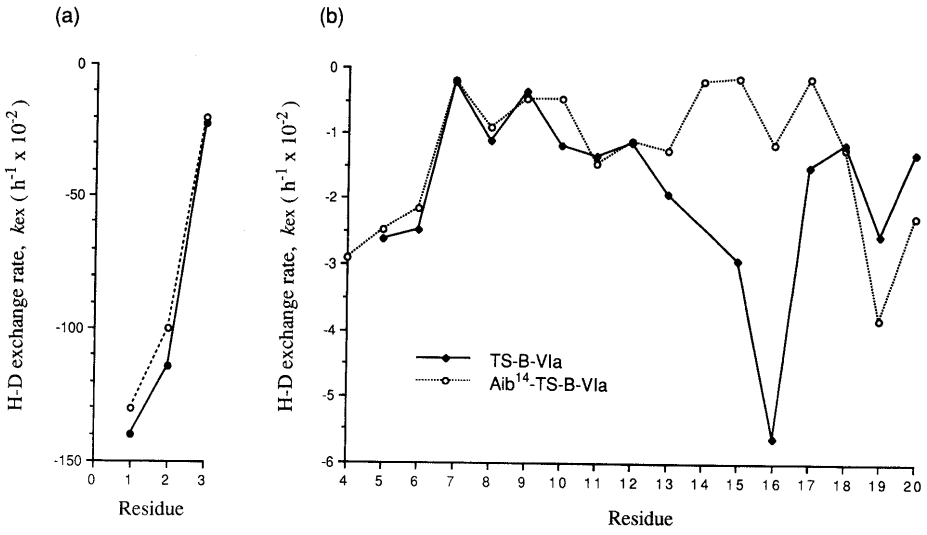

Fig. 5. Hydrogen-Deuterium (H-D) Exchange Rates of the Amide Protons at 293 K

Exchanging rates (k_{ex}) are defined as the slope of semilogarithmic plots of the decay of amide signal intensity versus the time (h) after dissolving the peptides in CD_3OD. Because of an overlap of the signals, the rate of Ala^{4}NH for TS-B-VIa was not detected. Note that the scales of k_{ex} for positions 1 to 3 (a) and for positions 4 to 20 (b) are different.

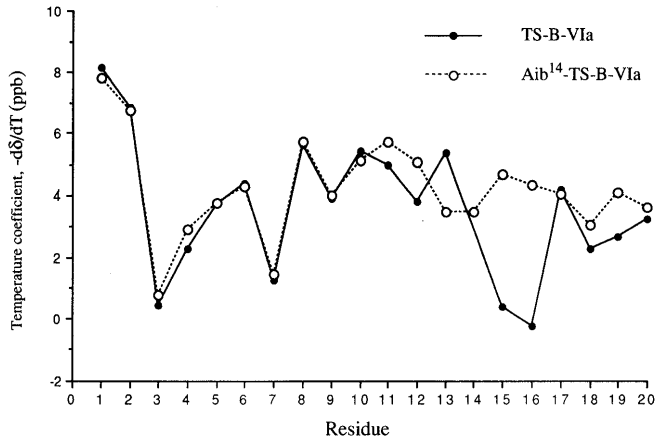

Fig. 6. Temperature Coefficients of NH Chemical Shifts for TS-B-VIa and Aib^{14}-TS-B-VIa Obtained over the Range of 286—307 K in CD_3OH

Positive $-d\delta/dT$ (ppb/K) values represent upfield shift of the NH signals with increasing temperature.

kinked structure in TS-B-VIa, minimizing repulsion between the imino ring of Pro^{14} and the Gly^{11} CO.[14,16]

The NH thermal coefficient values for the two peptides are shown in Fig. 6. Most values are small and negative (upfield shift with temperature increase). The values for both peptides at the N-terminal residues (Aib^1 NH-Aib^{10} NH) were similar, supporting the strong similarity of conformations of the two peptides in this region. The larger values for the Aib^1 NH and the Ala^2 NH of both peptides indicate that these NHs are not involved in the intramolecular H-bonding, but are exposed to the solvent. The Aib^3 NHs of both peptides and the Val^{15} NH and the Aib^{16} NH of TS-B-VIa show significantly small values. These NHs are involved in 1←4 H-bonding at the turning points from 3_{10}-helix to α-helix or α-helix to 3_{10}-helix. The small values would be due to the specific effects of these locations. The inter-residual H-bonding schemes proposed for TS-B-VIa and Aib^{14}-TS-B-VIa are illustrated in Fig. 7.

The Pro^{14}→Aib^{14} substitution of TS-B-VIa alters its C-terminal (Leu^{12} to Pheol^{20}) 3_{10}-helical conformation to α-helical conformation. Conversion of α-helix-Pro-3_{10}-helix structure to a long α-helix was also observed in phage T_4 lysozyme in which the Pro was replaced with any of seven other amino acids.[26] Several conformational studies of Aib-rich peptides have revealed that these peptides with less than eight residues preferentially form 3_{10}-helix, while α-helix was preferred by longer ones.[27,28] These observations are in agreement with the result that the 3_{10}-helix appears in the small C-terminal moiety (seven residues) following the kink around Pro^{14} in TS-B-VIa, whereas, owing to the lack of the Pro-kinked structure, α-helix is predominant in Aib^{14}-TS-B-VIa.

Both alamethicin[9] and TS-B-V[16] form an α-helix-kink(Pro^{14})-α-helix structure. In this structure, the polar Gln side chains and COs (Aib^{10} and Gly^{11}) not participating in inter-residual H-bonds align on one side of the helix. A single pore which is formed by a bundle of such helices seems to be the most probable form of voltage-gated ion-channel (Fig. 8a).[14] On the other hand, TS-B-VIa forms an α-helix-kink (Pro^{14})-3_{10}-helix structure. In this structure, the polar side chains of Gln^{18} and Gln^{19} should be located on the opposite side to the polar surface (δCONHs of Gln^7 and COs of Aib^{10} and Gly^{11}) of the N-terminal helical domain. If TS-B-VIa forms ion-channels by the bundle model, the conformation of TS-B-VIa seems disadvantageous to the amphiphilic properties and to the stabilization of the bundle of helices. However, considering that the bundle is placed perpendicular to the lipid bilayers, a bundle of α-helix-kink-3_{10}-helix could be stabilized by the interaction between C-terminal Gln side-chains and the polar region of lipid bilayers (Fig. 8b). Therefore, these polar side-chains could act as anchoring groups to the membrane surface.

Since Aib^{14}-TS-B-VIa forms an amphiphilic helix without a kinked structure, a bundle of such helices would suffer from steric hindrance owing to the bulky C-terminal residues. Furthermore, the bundle of Aib^{14}-TS-B-VIa lacks solvent-accessible carbonyls, such as Aib^{10} CO and Gly^{11} CO in TS-B-VIa, in the polar surface of the pore.

NII-Electronic Library Service

(a) TS-B-VIa

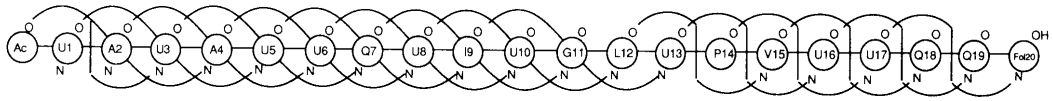

(b) Aib^{14}-TS-B-VIa

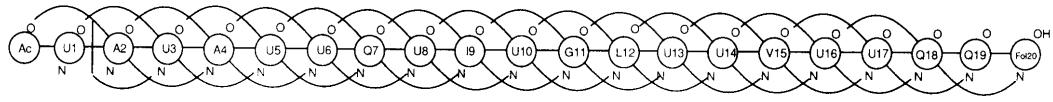

Fig. 7. Predominant Intramolecular Hydrogen Bonding Patterns for TS-B-VIa (a) and Aib^{14}-TS-B-VIa (b)

The one-letter code of amino acid residues is used with U = Aib, Fol = Pheol.

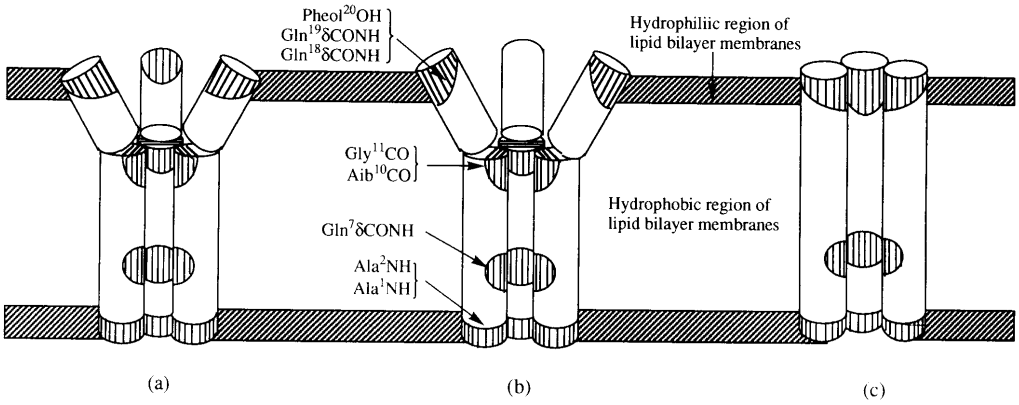

Fig. 8. Ion Channel Models Proposed for TS-B-VIa and Aib^{14}-TS-B-VIa

Polar parts (NHs of Aib^1 and Ala^2; δCONHs of Gln^7, Gln^{18}, and Gln^{19}; OH of Pheol^{20}; COs of Aib^{10} and Gly^{11}) of the peptide monomers are shown by oblique lines. The α-helix-kink-α-helix motif structure of alamethicin and TS-B-V (a) and the α-helix-kink-3_{10}-helix structure of TS-B-VIa (b) each form a funnel-shaped channel from a bundle of monomers. The Aib^{14}-TS-B-VIa channel is a bundle of straight cylindrical monomers (c).

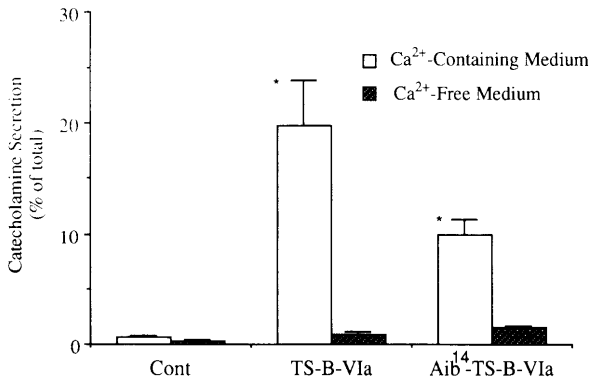

Fig. 9. Effects of TS-B-VIa and Aib^{14}-TS-B-VIa on Catecholamine Secretion from Cultured Bovine Adrenal Chromaffin Cells

The secretion was measured as previously described.[7] Adrenal chromaffin cells were isolated from bovine adrenal glands by collagenase digestion. The cells in modified Eagle's minimum essential medium were maintained at 37 °C in a CO_2 incubator and were used for experiments after 4 d of culturing. The cells were incubated for 10 min at 37 °C with 5 μM TS-B-VIa or Aib^{14}-TS-B-VIa in Ca^{2+}-containing or Ca^{2+}-free medium (plus EGTA). Catecholamine secretion is shown as a percentage of total cellular catecholamine content (191 ± 10 nmol). Data are means ± standard deviations from three experiments. The secretion was completely dependent on external Ca^{2+}. *, $p < 0.001$, significantly different from the control (Cont).

Consequently, the channel of Aib^{14}-TS-B-VIa would be more unstable than that of TS-B-VIa (Fig. 8c). Indeed, the catecholamine secretion-inducing activity of Aib^{14}-TS-B-VIa is less than that of TS-B-VIa, suggesting that the channel-forming ability of Aib^{14}-TS-B-VIa is lower than that of TS-B-VIa in the biomembranes (Fig. 9). The ion-channel-forming properties of these peptides will be discussed elsewhere.

Acknowledgements This work was supported in part by Grants-in-Aid for Scientific Research (05453180, 06303014, 06680558, and 06780467) from the Ministry of Education, Science and Culture of Japan.

References and Notes

1) Part XIX: Wada S., Iida A., Akimoto N., Kanai M., Toyama N., Fujita T., *Chem. Pharm. Bull.*, **43**, 910—915 (1995).
2) The following abbreviations are used: CD = circular dichroism; DQF-COSY = double quantum filtered correlation spectroscopy; EGTA = ethylene glycol bis(β-aminoethyl ether)-*N*,*N*,*N*′,*N*′-tetra-acetic acid; NOE = nuclear Overhauser effect; NOESY = nuclear Overhauser enhancement spectroscopy.
3) Fujita T., Iida A., Uesato S., Takaishi Y., Shingu T., Saito M., Morita M., *J. Antibiot.*, **41**, 814—818 (1988).
4) Iida A., Okuda M., Uesato S., Takaishi Y., Shingu T., Morita M., Fujita T., *J. Chem. Soc., Perkin Trans. 1*, **1990**, 3249—3255.
5) Brückner H., Przybylski M., *J. Chromatogr.*, **296**, 263—275 (1984).
6) Okuda M., Iida A., Uesato S., Nagaoka Y., Fujita T., Takaishi Y., Terada H., *Biol. Pharm. Bull.*, **17**, 482—485 (1994).
7) Tachikawa E., Takahashi S., Furumachi K., Kashimoto T., Iida A., Nagaoka Y., Fujita T., Takaishi Y., *Mol. Pharmacol.*, **40**, 790—797 (1991).
8) Nagaoka Y., Iida A., Kanbara T., Neoh L., Fujita T., Asami K., Asaka K., Tachikawa E., Kashimoto T., "Peptide Chemistry 1993," ed. by Okada Y., Protein Research Foundation, Japan, 1994, pp. 361—364.
9) Pandey R. C., Cook J. C., Jr., Rinehart K. L., Jr., *J. Am. Chem. Soc.*, **99**, 8469—8483 (1977).
10) Jung G., König W. A., Leibfritz D., Ooka T., Janko K., Boheim G., *Biochim. Biophys. Acta*, **433**, 164—181 (1976).
11) Bodo B., Rebuffat S., Hajji M. E., Davoust D., *J. Am. Chem. Soc.*, **107**, 6011—6017 (1985).

NII-Electronic Library Service

12) Matsuura K., Shima O., Takeda Y., Takaishi Y., Nagaoka Y., Fujita T., *Chem. Pharm. Bull.*, **42**, 1063—1069 (1994).
13) Wada S., Nishimura T., Iida A., Toyama N., Fujita T., *Tetrahedron Lett.*, **35**, 3095—3098 (1994).
14) Fox R. O., Jr., Richards F. M., *Nature* (London), **300**, 325—330 (1982).
15) Rebuffat S., Conraux L., Massias M., Aubin-Guette C., Bodo B., *Int. J. Peptide Protein Res.*, **41**, 74—84 (1993).
16) Iida A., Uesato S., Shingu T., Nagaoka Y., Kuroda Y., Fujita T., *J. Chem. Soc., Perkin Trans. 1*, **1993**, 375—379.
17) Nagaoka Y., Iida A., Fujita T., *Chem. Pharm. Bull.*, **42**, 1258—1263 (1994).
18) Marion D., Wüthrich K., *Biochem. Biophys. Res. Commun.*, **113**, 967—974 (1983).
19) Kumar A., Wagner G., Ernst R. R., *J. Am. Chem. Soc.*, **103**, 3654—3658 (1981).
20) Burgess A. W., Leach S. J., *Biopolymers*, **12**, 2599—2605 (1973).
21) Richardson J. S., Richardson D. C., *Science*, **240**, 1648—1652 (1988).
22) Wishart D. S., Sykes B. D., Richards F. M., *Biochemistry*, **31**, 1647—1651 (1992).
23) Wüthrich K., Billeter M., Braun W., *J. Mol. Biol.*, **180**, 715—740 (1984).
24) Wagner G., Neuhaus D., Wörgötter E., Vasak M., Kägi J. H. R., Wüthrich K., *J. Mol. Biol.*, **187**, 131—135 (1986).
25) Englander S. W., Kallenbach N., *Q. Rev. Biophys.*, **16**, 521—655 (1984).
26) Alber T., Bell J. A., Dao-Pin S., Nicholson H., Wozniak J. A., Cook S., Matthews B. W., *Science*, **239**, 631—635 (1988).
27) Karle I. L., Balaram P., *Biochemistry*, **29**, 6747—6756 (1990).
28) Toniolo C., Benedetti E., *Trends Biochem. Sci.*, **16**, 350—353 (1991).

NII-Electronic Library Service